SPECIAL ISSUE ARTICLE

JOR Spine OPEN ACCESS

Panax notoginseng saponins attenuate intervertebral disc degeneration by reducing the end plate porosity in lumbar spinal instability mice

Hao Hu[1] | Yan Chen[1] | Fangli Huang[1] | Bolin Chen[1] | Zhiyuan Zou[1] | Bizhi Tan[1] | Hualin Yi[1] | Chun Liu[2] | Yong Wan[1] | Zemin Ling[1] | Xuenong Zou[1]

[1]Department of Spine Surgery and Guangdong Provincial Key Laboratory of Orthopaedics and Traumatology, Sun Yat-sen University First Affiliated Hospital, Guangzhou, China

[2]Precision Medicine Institute, Sun Yat-sen University First Affiliated Hospital, Guangzhou, China

Correspondence
Xuenong Zou and Zemin Ling, Department of Spine Surgery and Guangdong Provincial Key Laboratory of Orthopaedics and Traumatology, Sun Yat-sen University First Affiliated Hospital, 58 Zhongshan 2nd Rd., Yuexiu District, Guangzhou 510080, China.
Email: zouxuen@mail.sysu.edu.cn (X. Z.) and lingzm3@mail.sysu.edu.cn (Z. L.)

Abstract

Although painkillers could alleviate some of the symptoms, there are no drugs that really cope with the intervertebral disc degeneration (IDD) at present, so it is urgent to find a cure that could prevent or reverse the progression of IDD. During the development of IDD, the cartilaginous end plates (EPs) become hypertrophic and porous by the increase of osteoclast activities, which hinder the penetration of nutrition. The compositional and structural degeneration of the EP may cause both nutritional as well as mechanical impairment to the nucleus pulposus (NP) so that developing drugs that target the degenerating EP may be another option in addition to targeting the NP. In the lumbar spine instability mouse model, we found increased porosity in the cartilaginous EP, accompanied by the decrease in total intervertebral disc volume. Panax notoginseng saponins (PNS), a traditional Chinese patent drug with anti-osteoclastogenesis effect, could alleviate IDD by inhibiting aberrant osteoclast activation in the porous EP. Further in vitro experiment validated that PNS inhibit the receptor activator of nuclear factor kappa-B ligand–induced osteoclast differentiation, while the transcriptional activation of PAX6 may be involved in the mechanism, which had been defined as an inhibitory transcription factor in osteoclastogenesis. These findings may provide a novel therapeutic strategy for IDD.

KEYWORDS
anti-osteoclastogenesis, end plate sclerosis, intervertebral disc degeneration, lumbar spine instability, Panax notoginseng saponins

1 | INTRODUCTION

Low back pain (LBP) is a common musculoskeletal disorder around the world, occurring in all ages from children to the elderly.[1] The number of disabled due to LBP increased by 54% from 1990 to 2015, and the

global prevalence of activity-limiting LBP reached 7.3% in 2015, imposing a huge social and economic burden worldwide.[2] The pathogenesis of LBP is complicated, and the intervertebral disc degeneration (IDD) is the primary pathological mechanism,[3] accounting for approximately 40% of all LBP cases.[4]

The nucleus pulposus (NP) of the intervertebral disc (IVD) is avascular throughout life, and its nutritional supply rely on the diffusion from the bony end plates (EPs) vascular network or blood vessels in the outer annulus fibrosis (AF).[5,6] The cartilaginous EP acts as a semipermeable barrier to control the exchange of nutrients or metabolic waste between the NP and the bony EP, which makes it very difficult for macromolecular drugs to diffuse into NP.[7] Besides, the axial pressure from vertebral body is first transmitted to the EP and then to the NP.[8] Therefore, the compositional and structural degeneration of the EP may cause both nutritional as well as mechanical impairment to the NP. Although, in most studies, the deterioration of NP tissue architectures were considered as the beginning and core issue of IDD,[9,10] our previous study found that degenerative changes in the EP may occur earlier than the NP, which could be quantified by T2 mapping, a special quantitative magnetic resonance imaging (MRI) sequence.[11] Thus, developing drugs that target the degenerating EP may be another option in addition to the strategy of targeting the NP.

The aberrant stress distribution caused by spine instability is one of the initial factor of IDD. The aberrant mechanical loading leads to lesions and inflammation within the EP, which could be described as modic changes in MRI imaging clinically.[12] If the inflammatory irritation persists, released cytokines and osteoclastic factors such as tumor necrosis factor alpha, interleukin 6, macrophage colony-stimulating factor, and receptor activator of nuclear factor kappa-B ligand (RANKL) could cause osteoclast activation and high bone turnover in the EP.[13] In a mouse lumber spine instability (LSI) model established by resection of partial posterior ligamentous complex, the abnormal bone remodeling results in increased porosity of the EP, which could be historically characterized by the surrounding tartrate-resistant acid phosphatase (TRAP$^+$) osteoclasts.[14] The porosity in the EP could subsequently exacerbate stress anomaly and nutrient diffusion disorder of the NP[15] and finally accelerate the whole IDD. Besides, a previous study has showed that osteoclasts within the porous EP induce sensory innervation by secreting Netrin-1, which mediates PGE2-induced spinal hypersensitivity and LBP in mice.[16] Thus, the activation of osteoclasts in the EP is a key part of the pathogenesis of IDD. Therefore, we speculate that the use of anti-osteoclastogenesis drugs targeting the degenerated EP may reduce the EP porosity and alleviate IDD.

Panax notoginseng (Burk) F. H. Chen, a widely used traditional Chinese medicine, has been evaluated with various pharmacological values,[17] such as anti-inflammatory,[18,19] anti-oxidation,[20] and inhibition of platelet aggregation,[21] whose main active ingredient is Panax notoginseng saponins (PNS). By using high-performance liquid chromatography and spectrophotometry, Ginsenosides Ra3, Rg1, Rb1, and Rd and notoginsenoside R1 were determined as main ingredients of the total saponins of Panax notoginseng.[22] After oral administration of PNS in rat, blood drug concentration of ginsenosides Ra3, Rb1, and Rd was significantly higher than other compounds.[23] Several studies had showed that PNS exert anti-osteoporosis effect in radiation-induced and ovariectomy-induced osteoporotic mice by dual action: stimulation of bone formation and inhibition of bone resorption.[24,25] Another study found that n-Butanol extracts of Panax notoginseng, which contained 24.1% ginsenoside Rb1 and 8.4% notoginsenoside R1, inhibited osteoclastogenesis in LPS-activated RAW264.7 cells by suppressing MAPK signaling pathway.[26] However, whether PNS could play a positive role in IDD remain unknown. In this study, we investigated whether PNS could prevent the loss of IVD volume in an LSI mouse model. And we hypothesized that PNS may reduce the EP porosity by inhibiting the osteoclastic activities and therefore attenuate IDD.

2 | MATERIALS AND METHODS

2.1 | Materials

PNS, the total saponins of Panax notoginseng, were purchased from KPC Xuesaitong Pharmaceutical Co. Ltd. (China); C57BL/6J mice were purchased from SPF Biotechnology Co. Ltd. (China); Raw 264.7 cells were purchased from ATCC (USA). Recombinant mouse TRANCE/RANKL/TNFSF11 (462-TEC) was purchased from R&D Co. Ltd. (USA); TRAP Staining Kit (294-67001) was purchased from Wako Co. Ltd. (Japan); culture and cytotoxicity assay (CCK-8) Cell Counting Kit (A311) was purchased from Vazyme Co. Ltd. (China); HiScript III First Strand cDNA Synthesis Kit (R312) was purchased from Vazyme Co. Ltd. (China); ChamQ SYBR qPCR Master Mix (Q311) was purchased from Vazyme Co. Ltd. (China); PAX6 antibody (#60433) was purchased from Cell Signaling Technology, Inc. (USA); Poly-HRP secondary antibody (PR30009) was purchased from Proteintech Group, Inc. (USA); DAB (ZLI-9017) was purchased from ZSGB-BIO Co. Ltd. (China).

2.2 | LSI model and PNS treatment

The animal study was approved by the Institutional Review Board and Animal Care Committee of Guangzhou Huateng Bio-medical Technology Co., Ltd (Approval Number: HTSW201014), and the samples were further analyzed in the First Affiliated Hospital of Sun Yat-sen University. Thirty 12-week-old female C57BL/6J mice were housed in individual ventilated cages under controlled conditions (temperature, 20-26°C; humidity, 40%-70%) for a 12-hour light-dark cycle and were allowed free access to water and food. After 1-week adaptation period, 30 mice were randomly divided into five equal groups (six in one cage): (1) Sham operation group, (2) LSI mouse model, (3) LSI + low dose (40 mg/kg/d) PNS, (4) LSI + middle dose (80 mg/kg/d) PNS, and (5) LSI + high dose (160 mg/kg/d) PNS. LSI and sham operation were performed under pentobarbital sodium (90 mg/kg, ip) anesthesia. In each mouse, a longitudinal incision was made in the middle

of the back. While sham operation group was only detached the posterior paravertebral muscles from the lumbar second to fifth vertebrae (L3-L5) vertebrae, classical LSI model was established by resecting partial spinous process, the spinous, supraspinous, and interspinous ligaments from the L3-L5 vertebrae (Figure 1B).[14]

One week after the operation, mice in PNS-treated groups were orally administered with different dosages for 8 weeks, while mice in the sham group and the LSI group were also orally administered with normal saline in the same volume (0.4 ml equally in each group) according to in vivo experiment design (Figure 1A). In clinics, the recommended dose of PNS for human adults is 150-600 mg/d so that the translation dosage for mice is approximately 30-120 mg/kg/d according to the body surface area normalization method.[27] In this study, we applied 40 and 80 mg/kg/d as low and middle doses, which were within the recommended dose range. And we also applied a high dose of 160 mg/kg/d, which was a little higher than the recommended maximum dose (120 mg/kg/d) and had been reported in previous study.[25]

After 8-week PNS treatment, all mice were euthanized. PBS and paraformaldehyde were perfused into the whole body through the left ventricle. The lower thoracic, whole lumbar spine, and part of sacrum from mice were dissected and stored at 4% paraformaldehyde at 4°C. For the next microcomputed tomography (micro-CT) and histological analysis, IVDs from L2/L3, L3/L4, and L4/L5 in each mice were used for examination. So that in each cohort, six mice with 18 IVD samples were examined. Eight weeks after operation, LSI lumbar spines exhibited narrower intervertebral space than sham

control (Figure 1C), which indicates the IDD LSI mouse model was established successfully.

2.3 | Micro-CT scanning and analysis

Each lumbar spine from mice was scanned using a desktop Micro-CT SkyScan1275 (Bruker Micro CT, Belgium). The micro-CT scanner was operated at a voltage of 49 kVp and a current of 200 μA to measure the IVD and cartilage EP. And the spatial scanning resolution was set at 6.8 μm per pixel for optimal image contrast. Coronal and sagittal images of the L2-L5 IVD were used to reconstruct and process for three-dimensional histomorphometric analyses of IVD and cartilage EP through softwares NRecon and DataViewer (Bruker micro-CT, Belgium). Three-dimensional model analyses of spine were carried out using software CTvox (Bruker micro-CT, Belgium) while three-dimensional image analyses of IVD and cartilage EP were reconstructed with software CTAn (Bruker micro-CT, Belgium). To further examine the degeneration of different regions, all IVDs (L2/3-L4/L5), and adjacent upper (toward the head), lower (toward the tail) EPs were divided into ventral (toward the abdomen), middle, and dorsal (toward the back) sections for the analysis (Figure 1B,C). IVD volume was defined by a free-drawing region of interest (ROI) that cover the whole invisible space between each lumber vertebrae. EP volume was defined by a free-drawing ROI that was positioned over the visible bony plate close to the vertebral body, separated by the growth plate. Then, the tissue volume (mm^3; TV) of IVD and the bone volume
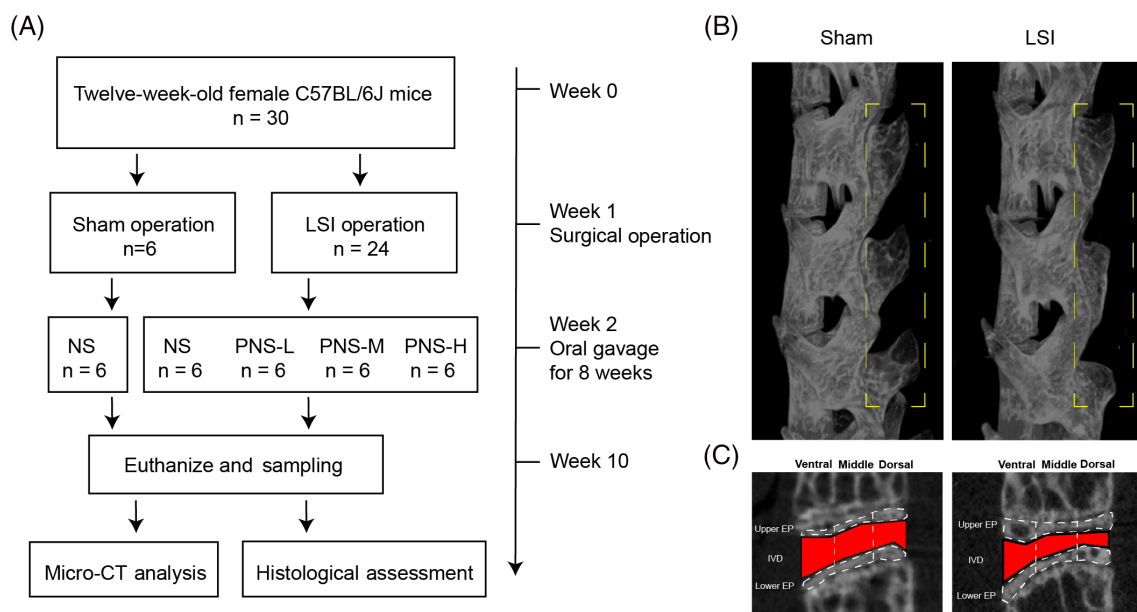

FIGURE 1 Lumbar spine instability (LSI) mouse model and in vivo experiment. (A) Protocol design for in vivo experiment. (B) Sagittal view of micro-CT reconstructed volume blending image of lumbar spine. The spinous process and the adjacent soft tissues (yellow-dotted line area) were resected in the LSI model. (C) Sagittal view of micro-CT reconstructed image of intervertebral disc (IVD) volume and adjacent end plates. All IVDs (red area) and upper end plates and lower end plates (dotted area) were divided into ventral, middle, and dorsal sections for analysis, respectively. Micro-CT, Microcomputed tomography; NS, normal saline; PNS, Panax notoginseng saponins; PNS-H, 160 mg/kg/d; PNS-L, 40 mg/kg/d PNS; PNS-M, 80 mg/kg/d

fraction (BV/TV; %) or porosity (1-BV/TV; %) of cartilage EP were calculated by assigning a threshold content within 90 continuous slices through software CTAn (Bruker micro-CT, Belgium), which was used to analyze parameters to measure the IVD and cartilage EP. Finally, three-dimensional models of volume of interest were reconstructed with model visualization software CTVol (Bruker micro-CT, Belgium) for morphologic measurements. The operators and researchers conducting the micro-CT analysis were both blinded to the treatments associated with samples.

2.4 | Histological assessment

After micro-CT analysis, all spine specimens were prefixed at 4% paraformaldehyde for 48 hours, decalcified in 10% EDTA (pH 7.4) for 21 days at 4°C, dehydrated and embedded in paraffin; 4-μm-thick coronal-oriented (longitudinally) sections of L2-L5 were processed. Safranin O-Fast Green staining was performed for the analysis of IVD microstructure. TRAP staining for sections of the lumbar of each mouse was performed using a standard protocol to identify activated osteoclasts (TRAP Staining Kit, Wako Co. Ltd., 294-67001).[28] The images were observed and captured by an image scanning microscope (Leica, Germany). The TRAP$^+$ cells were obtained by counting the number of positive staining cells in the cavities of the EP region. And then, we applied a quantitative mouse IVD histopathological scoring system to evaluate the IDD from Safranin O-Fast Green sections.[29] The scoring system analyzed 14 key histopathological features from NP, AF, EP, and AF/NP/EP interface regions. The total score ranges from 0 to 36, classifying normal (0-6), mild (7-13), moderate (14-25), and severe IDD (26-35). Two blinded raters scored each image independently, and average of the two raters was used for further analysis. For immunochemistry, the sections were incubated at 4°C overnight with primary antibodies anti-PAX6 (#60433, Cell Signaling Technology, 1:200); the Poly-HRP secondary antibodies (PR30009, Proteintech Group) were added onto the sections for 1 hour at room temperature; slides were stained with DAB (ZLI-9017, Origene) and then counterstained with hematoxylin (Sigma-Aldrich).

2.5 | In vitro osteoclast CCK8

Raw264.7 were monocyte/macrophage-derived cells, obtained from ATCC. Cells were cultured in Dulbecco's modified Eagle medium (high glucose formulation) containing 10% fetal bovine serum and 1% penicillin/streptomycin and then stay in a humidified environment of 5% carbon dioxide, 21% oxygen, and 37°C environment. Cells were seeded in a 96-well plate at a density of 5×10^3 cells/well in 100 μl of culture medium in an incubator at 37°C. After 24 hours, the culture medium was refreshed with different concentration of PNS (0, 0.1, 0.2, 0.4, 0.8, and 1.6 mg/ml), referring to previous studies.[24,30,31] In the next 24, 48, and 72 hours, 10 μl of CCK8 solution was added to each well using a repeating pipettor. After Incubating for 2 hours in the incubator, the absorbance of each well was measured at 450 nm using a microplate reader (BioTek).

2.6 | In vitro osteoclast differentiation and real-time quantitative polymerase chain reaction (RT-qPCR) Assays

Raw264.7 cells were seeded in six-well plates (1×10^5 cells/well) for 24 hours and then were stimulated with 50 ng/ml RANKL for 7 days to induce osteoclastogenesis. To verify inhibitory effect of PNS on osteoclastogenesis, cells in six-well plates were treated with or without PNS (0.4 mg/ml) and were divided into three groups: (1) Blank control group, (2) RANKL group, and (3) RANKL + PNS (0.4 mg/ml) group. The medium was refreshed every 2 days, and after 7-day induction, the total RNA was extracted using TRIzol reagent, and HiScript III First Strand cDNA Synthesis Kit was used for reverse

TABLE 1   Primer sequences used for real-time PCR

Gene	Forward primer sequence (5′-3′)	Reverse primer sequence (5′-3′)
CTSK	CTCGGCGTTTAATTTGGGGAGA	TCGAGAGGGAGGTATTCTGAGT
MMP9	GCAGAGGCATACTTGTACCG	TGATGTTATGATGGTCCCACTTG
NFATC1	GGAGAGTCCGAGAATCGAGAT	TTGCAGCTAGGAAGTACGTCT
PAX6	CTTCAGTACCAGGGCAACCC	TGGCCCTTCGATTAGAAAACCA
GAPDH	GCTCACTGGCATGGCCTTCCG	GTGGGCCATGAGGTCCACCAC

Abbreviations: CTSK, Cathepsin K; GAPDH, glyceraldehyde 3-phosphate dehydrogenase; MMP9, matrix metallopeptidase 9; NFATC1, nuclear factor of activated T cells 1; PAX6, paired box protein; PCR, polymerase chain reaction.
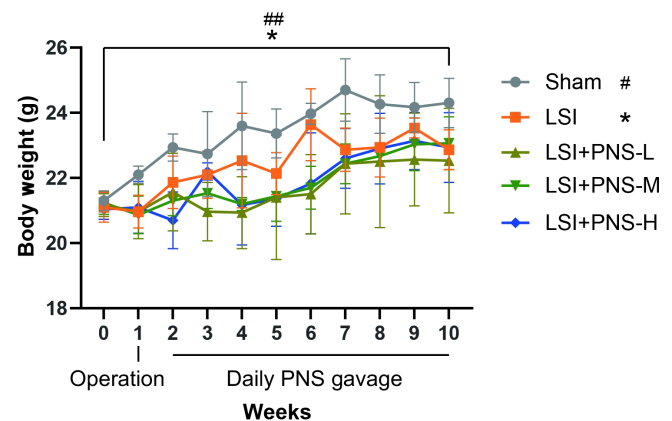

FIGURE 2   Body weight of mice in vivo experiment. Significance was determined using repeated measures one-way analysis of variance with post hoc Tukey honestly significant difference test. LSI, Lumber spine instability; PNS, Panax notoginseng saponins; PNS-H, 160 mg/kg/d; PNS-L, 40 mg/kg/d PNS; PNS-M, 80 mg/kg/d. Body weight of 10 weeks vs 0 week, ##$P < .01$; *$P < .05$

transcription to generate cDNA. cDNA was used as a template for RT-qPCR analysis using the ChamQ SYBR qPCR Master Mix according to manufacturer's protocols, and glyceraldehyde 3-phosphate dehydrogenase was used as the internal reference. Relative mRNA expression of target genes was calculated using the $2^{-\Delta\Delta Ct}$ method. The primer sequences used are shown in Table 1.
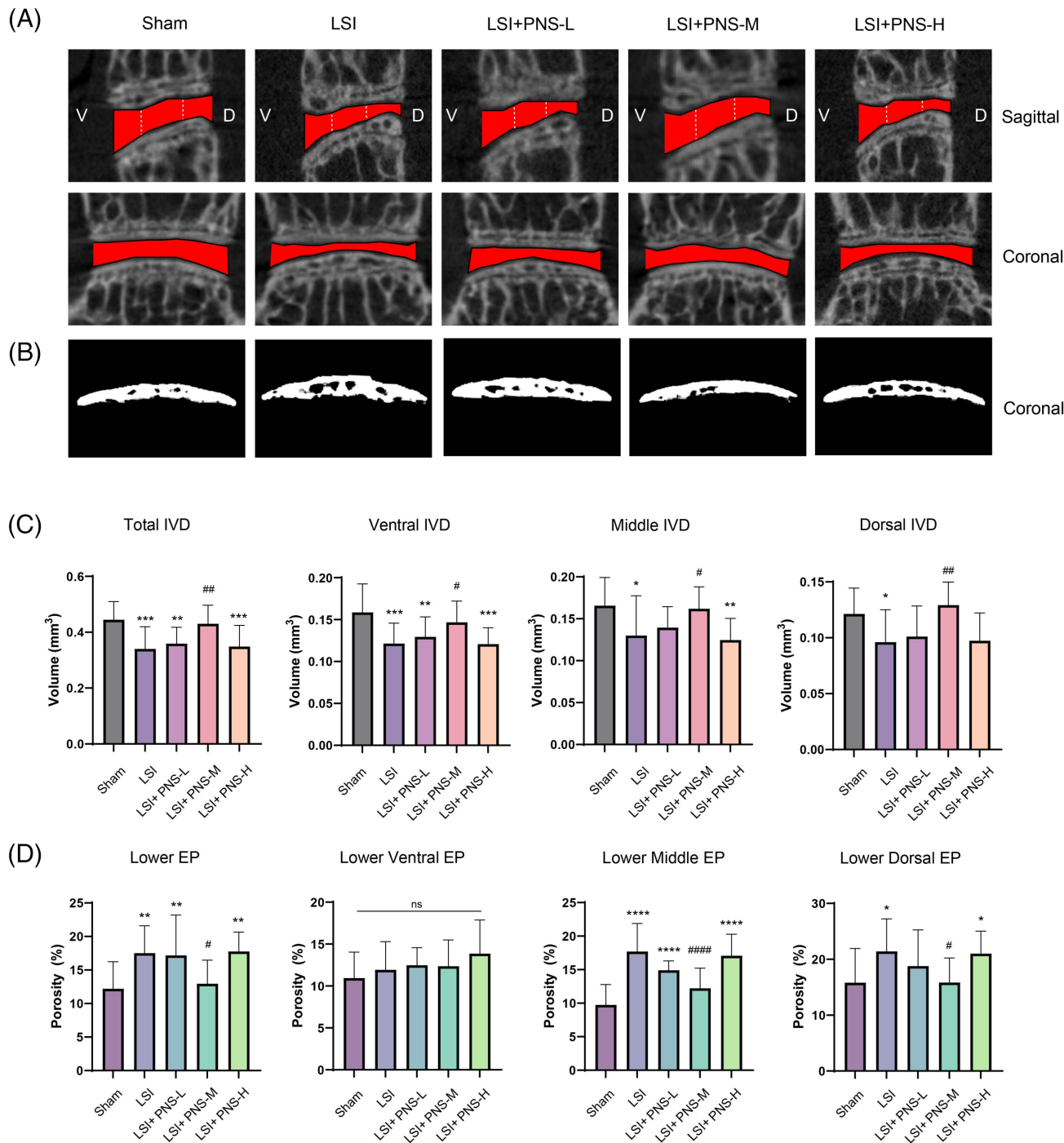

FIGURE 3 PNS increased lumbar intervertebral disc volume and reduced lower end plate porosity. (A) Representative view of reconstructive intervertebral disc (IVD) volume showed PNS increased IVD volume (red area) in LSI mouse model. White dotted line separates intervertebral disc and adjacent end plates into three equal section, dorsal, middle, and ventral, respectively, for analysis. (B) Coronal view of 3D reconstructed image of adjacent lower middle end plates showed PNS reduced lower end plate porosity in LSI mouse model. (C) PNS, especially PNS-M increased IVD volume in LSI mouse model. (D) PNS-M reduced end plate porosity in LSI mouse model. D, Dorsal; EP, end plate; LSI, lumbar spine instability; ns, no significance; PNS, Panax notoginseng saponins; PNSH, 160 mg/kg/d; PNS-L, 40 mg/kg/d PNS; PNS-M, 80 mg/kg/d; V, ventral. Significance was determined using one-way analysis of variance with post hoc Tukey honestly significant difference test. LSI and PNS-treated groups vs sham, $*P < .05$; $**P < .01$; $***P < .001$; $****P < .0001$. PNS-treated groups vs LSI, $\#P < .05$; $\#\#P < 0.01$; $\#\#\#P < .001$; $\#\#\#\#P < .0001$

2.7 | Statistic

All data analyses were performed using Prism software (Version 9.1.0). Data are presented as means ± standard deviations. For comparisons between five groups' quantitative data, we used one-way analysis of variance with post hoc Tukey honestly significant difference test after the evaluation of normal distribution and homogeneity of variance. For comparisons between five groups' qualitative data, we used χ^2 (and Fisher's exact) tests. For all experiments, $P \leq .05$ was considered to be significant. All inclusion/exclusion criteria were preestablished, and no samples or animals were excluded from the analysis. No statistical method was used to predetermine the sample size. The experiments were randomized, and the investigators were blinded to allocation during experiments and outcome assessment. The same sample was not measured repeatedly.

3 | RESULTS

3.1 | PNS treatment attenuates IVD volume loss and reduces the EP porosity in LSI model

In this study, we first examine whether PNS treatment can alleviate or postpone lumbar spine, especially EP and IDD in vivo by using an LSI mouse model. As the procedure aforementioned, all animals underwent satisfactory anesthesia, proper surgical handling, and hematischesis during operation to ensure postoperative recovery, no wound infection and death were observed throughout the in vivo experiment. There's no significant difference in mice's behavior and activities compared with those before operation. All mice showed a consistent, slightly increasing body weight during the observed period (Figure 2). However, mice in sham and LSI group gained significantly increased body weight than those in the PNS-treated groups after housing for 10 weeks. We inferred that daily gavage of PNS may have a negative impact on the appetite of mice, resulting in less significant body weight gain than those in PBS-treated groups. However, no significant body weight difference is observed between groups at every time points in this study.

Progressively more porous EPs with narrowed IVD space are major characteristics of IDD.[32][33] Analysis of LSI EPs by micro-CT scanning showed decreased IVD volume and height of intervertebral space as well as increased EP porosity in comparison with sham-control 9 weeks after operation (Figure 3A,B). After oral administration of PNS for 8 weeks, LSI lumbar spines showed generally higher IVD volume and intervertebral space than LSI-operated control. Importantly, PNS-M (80 mg/kg/d) group showed
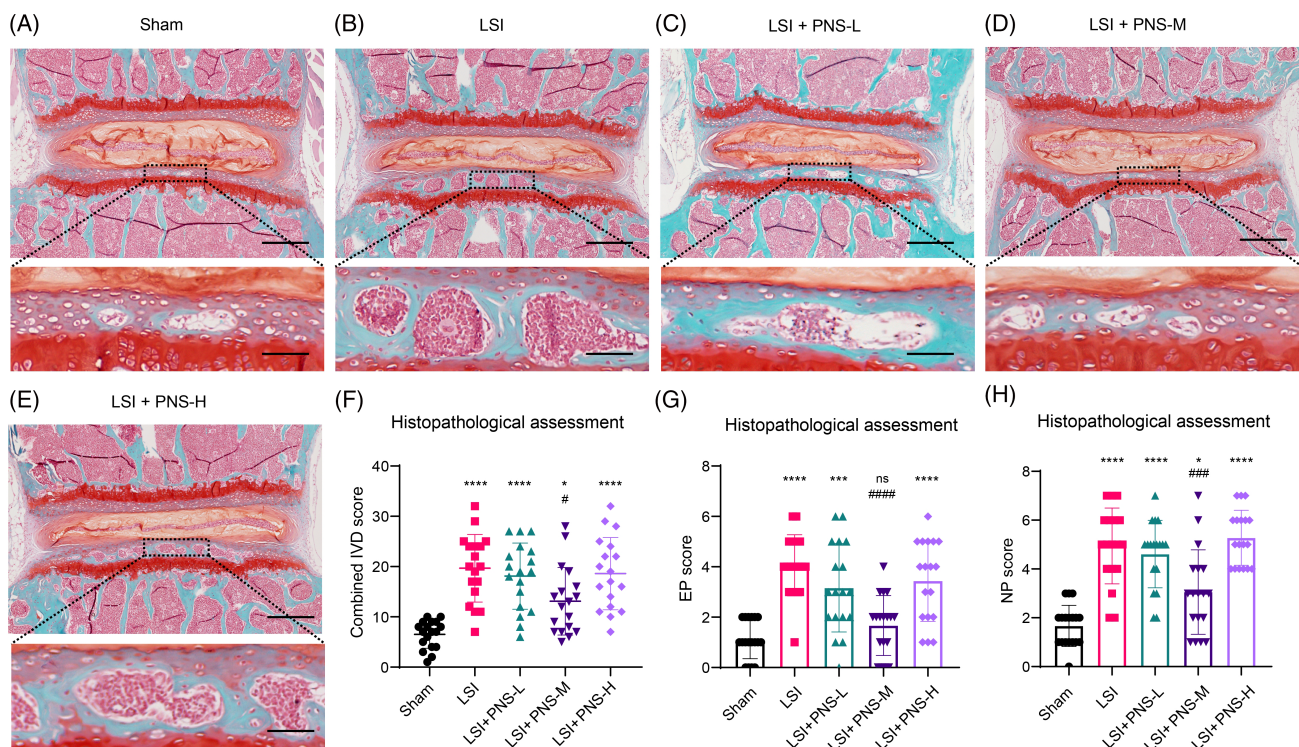

FIGURE 4 PNS inhibits lumbar intervertebral disc and end plate degeneration. Coronal sections of IVD and end plate stained by Safranin O/Fast Green in sham group (A), LSI group (B), LSI + PNS-L group (C), LSI + PNS-M group (D), and LSI + PNS-H group (E), red indicates proteoglycan, green/blue stains calcified cavities. (F-H) Combined IVD score, EP score, and NP score of each group. Scale bar in A-E represents 500 μm (upper image) and 100 μm (lower image), respectively. Quantitative measurements represent mean ± SD. Significance was determined using one-way analysis of variance with post hoc Tukey honestly significant difference test. EP, End plate; IVD, intervertebral disc; LSI, lumbar spine instability; NP, nucleus pulposus; PNS, Panax notoginseng saponins; PNS-H: 160 mg/kg/d; PNS-L: 40 mg/kg/d PNS; PNS-M: 80 mg/kg/d. LSI and PNS-treated groups vs sham, *$P < .05$; **$P < .01$; ***$P < .001$; ****$P < .0001$. PNS-treated groups vs LSI, #$P < .05$; ##$P < .01$; ###$P < .001$; ####$P < .0001$
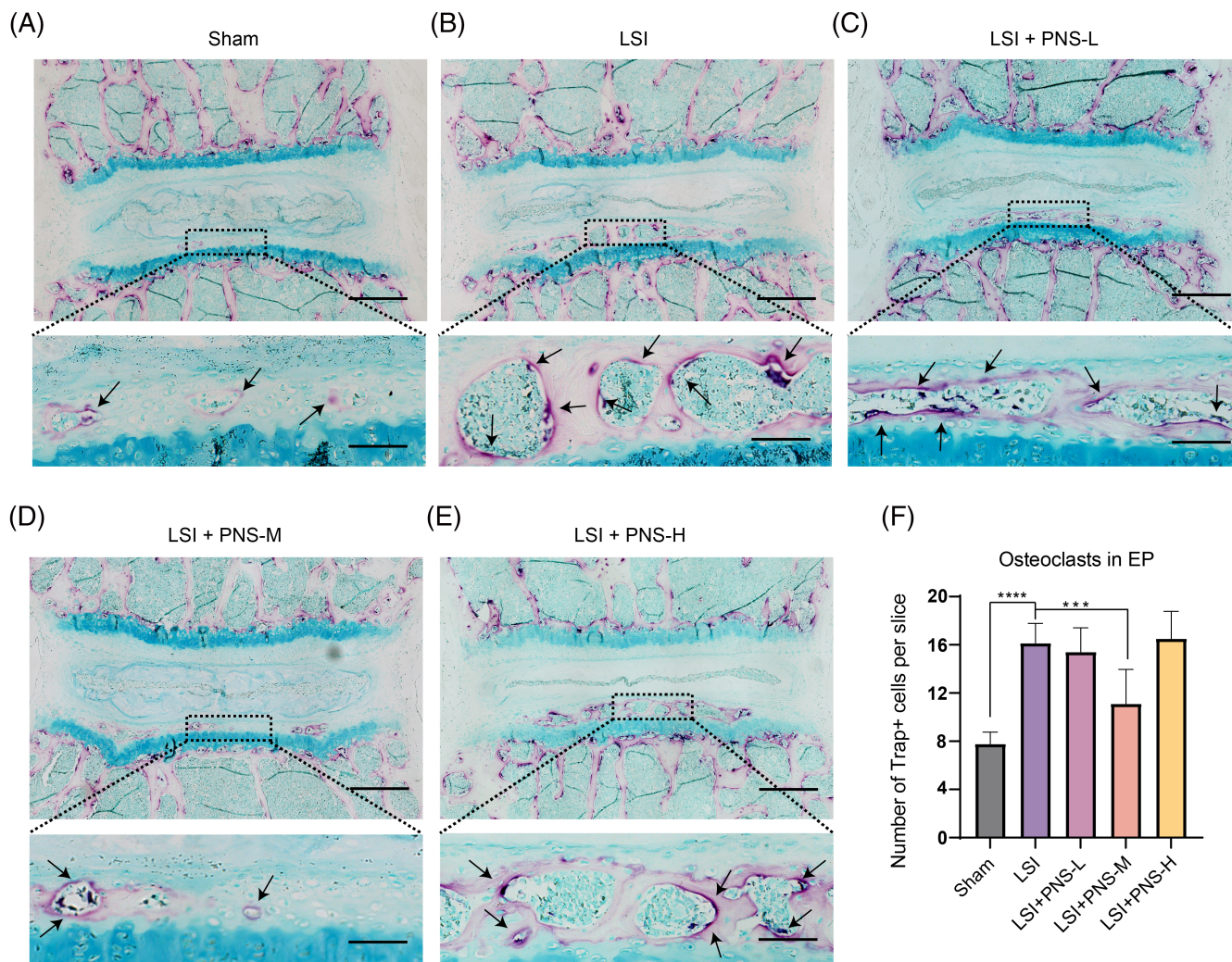
FIGURE 5 PNS inhibits osteoclast activity in LSI lower end plates. Coronal sections stained by TRAP of end plate in sham animals (A), LSI animals (B), LSI + PNS-L animals (C), LSI + PNS-M animals (D), and LSI + PNS-H animals (E). Violet represents TRAP staining positive. (F) Counting of TRAP (+) staining cells (black arrow). Scale bar in A-E represents 500 μm (upper image) and 100 μm (lower image), respectively. Quantitative measurements represent mean ± SD. Significance was determined using one-way analysis of variance with post hoc Tukey honestly significant difference test. EP, End plate; LSI, lumbar spine instability; PNS, Panax notoginseng saponins; PNS-H: 160 mg/kg/d; PNS-L, 40 mg/kg/d PNS; PNS-M, 80 mg/kg/d; TRAP, tartrate-resistant acid phosphatase. ***$P \leq .001$; ****$P \leq .0001$

significantly higher total IVD volume and lower EP porosity rate than LSI group, similar to those of the sham-control (Figure 3C,D). In addition, PNS-M showed effective decrease only in lower middle and dorsal EP porosity but not in lower ventral EP. However, no significant difference was found in upper EP between each group (data not shown). Meanwhile, the effect of PNS on LSI degenerative spine wasn't entirely dose dependent, low dose (40 mg/kg/d) showed mild effect on IVD and lower EP recovery without significance, while high dose (160 mg/kg/d) had no effect on both. Thus, PNS with appropriate dose (80 mg/kg/d) plays a preventive role in IVD volume decrease and EP porosity increase in LSI mouse. All the statistical parameters of IVD volume and EP porosity rate of each cohort could be found in Tables S1 and S2.

3.2 | PNS delay IDD by inhibiting aberrant osteoclast activation in sclerotic EP

The LSI mouse model develops lumbar IDD by increasing porosity and hypertrophy in EPs at an early stage, decreasing IVD volume, shrinkage in NP at later period.[14] Our micro-CT analysis has indicated recovery of microstructure in EP and IVD volume in PNS-M group. Thus, to further examine the effect of PNS on LSI model, we mainly focused on pathological changes in L2/3-L4/5 IVDs and adjacent lower EPs. Safranin-O/Fast Green staining of coronal sections of LSI and LSI + PNS IVD and EP evidenced disc degeneration of varying severity in comparison with sham control. NP tissue degeneration was characterized by increased matrix fibrosis, less NP cells, and
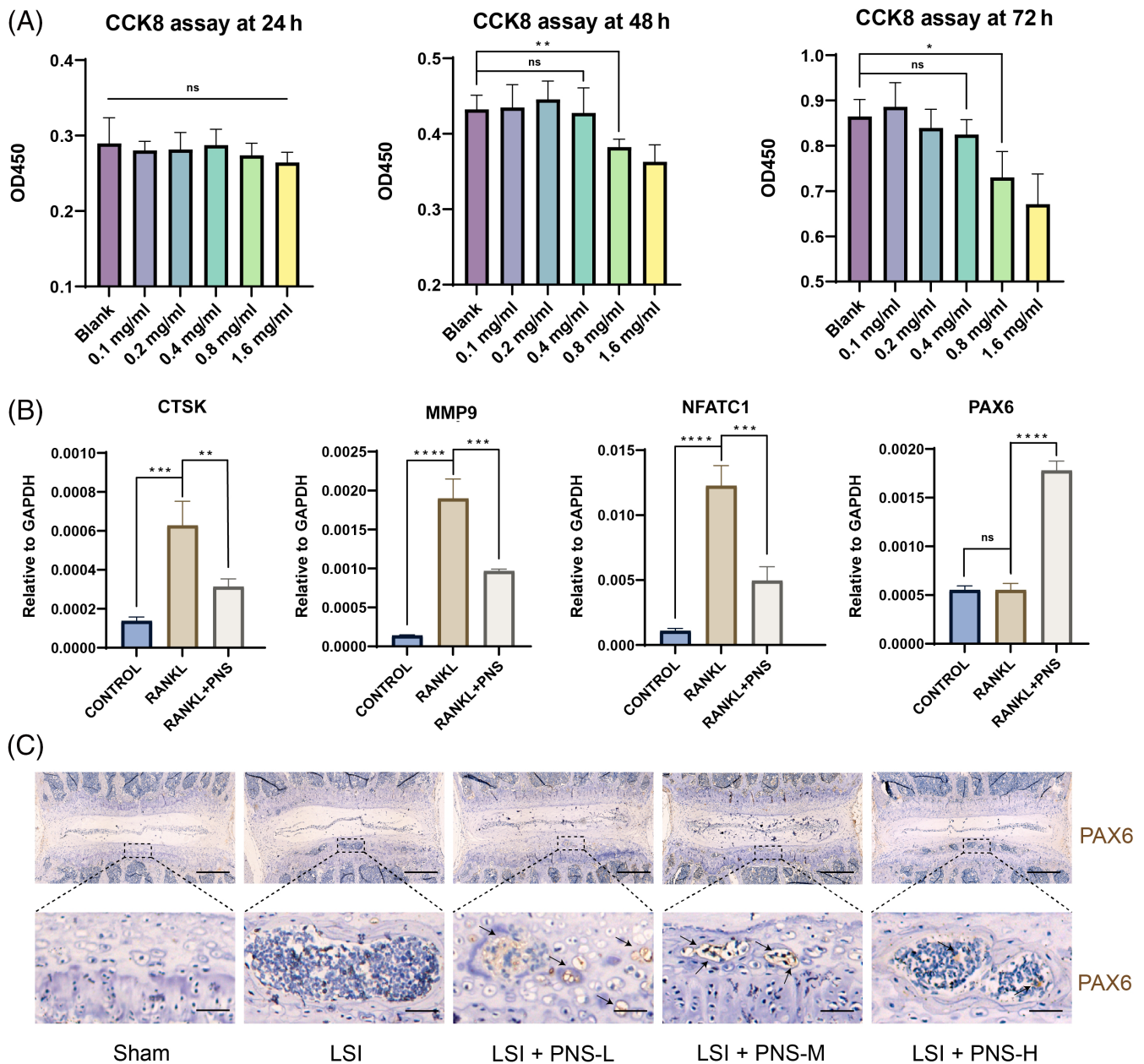
FIGURE 6 PNS inhibits osteoclastogenesis in vitro. (A) Cytotoxicity assay of PNS against RAW264.7 at different concentrations. (B) Quantitative analysis of the expression of Cathepsin K (CTSK), matrix metallopeptidase 9 (MMP9), nuclear factor of activated T cells 1 (NFATC1), and paired box protein (PAX6) in RAW264.9 at Day 7 determined by qRT-PCR. (C) Immunohistochemistry staining of PAX6 (black arrow) in IVD sections. Scale bar in A-E represents 500 μm (upper image) and 100 μm (lower image), respectively. Quantitative measurements represent mean ± SD. Significance was determined using one-way analysis of variance with post hoc Tukey honestly significant difference test; CCK8, Culture and cytotoxicity assay; LSI, lumbar spine instability; ns, not significant; PNS, Panax notoginseng saponins at 0.4 mg/ml; PNS-H, 160 mg/kg/d; PNS-L, 40 mg/kg/d PNS; PNS-M, 80 mg/kg/d; qRT-PCR, real-time quantitative polymerase chain reaction; RANKL, receptor activator of nuclear factor kappa-B ligand at 50 ng/ml. **$P \leq .01$; ***$P \leq .001$; ****$P \leq .0001$

rearrangement of cells into a honeycomb-like pattern (Figure 4B,C,E). Discs with degeneration showed loss of Safranin-O and less NP cells in the narrower NP compartment, suggesting fibrosis of the matrix and loss of proteoglycan. In addition, a demarcation between normal cartilage EP (CEP) and growth plate (GP) was evident with clear ossification of CEP stained by fast green as well as porous bone marrow cavity (Figure 4B-E). Although LSI model developed more calcification

in the lower EP, with oral administration of PNS, especially with medium dose (PNS-M, 80 mg/kg/d), porosity of the EP and formation of bone marrow cavities in sclerotic EP were reduced significantly (Figure 4B-E). In line with a quantitative mouse IVD histopathological scoring system previously described to evaluate the whole degenerative IVD,[29] we scored the NP, AF, EP, and AF/NP/EP boundary regions in every single IVD of each group. The combined IVD score

showed that all of the LSI operation groups had a significant higher score than the sham operation group, while the PNS-M-treated group scored slightly lower than the LSI group (Figure 4F). Specifically, PNS-M treatment had lower EP and NP score than LSI group but showed no difference in AF and boundary regions (Figure 4G-H and Table S3). Taken together, PNS-M treatment reduced cavities in sclerotic EP and attenuated the degeneration of the whole IVD, especially in the NP and EP regions.

The formation of cavities in degenerative EP and sensory nerve innervation are closely related to the activation of osteoclasts by spinal instability.[14,34] PNS were proved capable of suppressing osteoclast turnover and bone resorption in vivo.[24,35] We sought to demonstrate whether PNS inhibit the cavity formation in sclerotic EP by affecting osteoclast activity and bone resorption. Coronal sections of instable spines showed that aberrant osteoclast activity of bone resorption in the sclerotic EP inner cavity wall was significantly higher than that in the sham control (Figure 5A,B). Medium-dose PNS (PNS-M, 80 mg/kg/d) also evidently inhibited activation of osteoclast (Figure 5D), which was confirmed by TRAP (+) cell counting (Figure 5F), in consistence with less porosity and bone marrow cavities in the sclerotic EPs. Low (40 mg/kg/d) and high (160 mg/kg/d) dose did not show any improvements. These results verified the suppression of osteoclast activity is the key process for PNS to delay the degeneration of the sclerotic EP.

3.3 | PNS suppress osteoclastogenesis in vitro

Previous studies showed that PNS exert anti-osteoclastogenesis effect in LPS-induced RAW264.7 cells in vitro; however, its potential mechanism has not been revealed. We first evaluated the optimized concentration of PNS in vitro against RAW264.7 cells. CCK8 cytotoxicity assays indicated coculture with PNS alone at concentrations of 1.6 mg/ml or lower for 24 hours did not affect RAW264.7 cell viability, but the viability decreased at a concentration of 0.8 mg/ml at 48 hours (Figure 6A) or more. Thus, we used 0.4 mg/ml as the optimal concentration. We further observed the effect of PNS on the expression of osteoclastogenic marker genes, including Cathepsin K, matrix metallopeptidase 9, nuclear factor of activated T cells 1 (NFATC1), and paired box protein, in RAW264.7 after cocultured with or without RANKL or RANKL+PNS using qRT-PCR (Figure 6B). Matrix degradation–related genes, including CTSK, MMP9, and well-known osteoclastogenic transcription factor NFATC1 were all significantly lower in RANKL coculture with 0.4 mg/ml PNS than those with RANKL alone, which demonstrated osteoclastogenesis was inhibited by PNS in vitro. Surprisingly, the recently known anti-osteoclastogenic transcription factor PAX6 was over 3-fold higher in RANKL+PNS than RANKL alone, suggesting PAX6 plays an essential role in PNS' anti-osteoclastogenic effect. Immunochemistry of PAX6 in the IVD sections also showed PNS treatment increased PAX6 expression in the cavities of the EPs while no differences were observed in NP and AF cells (Figure 6C).

4 | DISCUSSION

Currently, there are no drugs that cope with the IDD in the clinic, and the ultimate solution for IDD patients is spinal fusion, so it is urgent to find a cure that could delay or reverse the progression of IDD. During the development of IDD, aberrant bone remodeling emerges in the EP, resulting in abnormal mechanical stress and nutritional disturbance of the NP. In the LSI model, TRAP[+] osteoclasts appear in the cavities within the degenerate EP, which could lead to sensory innervation in porous EPs by secreting Netrin-1, one of the axon-guidance molecules.[27] Therefore, inhibiting the aberrant osteoclasts activities within the EP may be an effective way to treat IDD.

In this study, 8 weeks after the LSI surgery, mice showed significant reduction in IVD volume, accompanied by obvious porosity in the cartilage EP. While most studies do not analyze the upper and lower EP separately, we observed that the degenerate porosity changes only occurred in the lower EP between the LSI group and sham operation group, particularly in the lower middle EP and lower dorsal EP. Interestingly, our previous study in rhesus monkeys found that lower EP degeneration was positively associated with NP degeneration, especially in the lower middle EP.[15] These may explain why the lower EP is more vulnerable than upper EP, which has been confirmed by several studies.[36,37] In our LSI model, the posterior ligamentous complex and spinous process were removed, so the axial stress would be more concentrated on the lower middle and dorsal EP, which explains why the lower ventral EP did not develop degenerate changes. After the LSI surgery, we applied PNS, a drug with anti-osteoclastic activity for preventive therapy. It showed that medium doses of PNS (80 mg/kg/d) were effective in reducing the porosity rate and osteoclasts count in the lower EP and restoring IVD volume. The lack of therapeutic effect at low doses (40 mg/kg/d) may be due to the low blood concentration reaching the EP while the lack of therapeutic effect at high-dose PNS (160 mg/kg/d) may be due to the cytotoxicity at high blood concentration, which had been confirmed in our previous study that high-dose PNS intake could impair liver and kidney function to some extent.[25] It is also possible that the high dose of PNS caused toxicity to the NP cells, but the present study failed to test whether the effective constituent of PNS could penetrate through the cartilage EP to reach the NP, which is a major limitation of this paper. In addition, it is important to note that we only applied female mice in this study mainly to reduce the animal individual difference. Although it's still unclear whether gender has an effect on disc degeneration,[38,39] the findings of this study are currently limited for females.

Another limitation comes from the animal model. Although previous study had considered mouse lumbar IVD as the animal model most geometrically similar to the human IVD,[40] no animal model can perfectly simulate the IDD because of the inherent complexity of the human IVD. The notochordal cells in human are completely absent from the NP by early adulthood, but in mice, they persist throughout life.[41] Besides, human IVDs bear much more mechanical forces than quadrupedal animal due to the upright posture; thus, whether the PNS treatment could work in human require more evidence from

bipedal primates animal (eg, rhesus monkey) experiments and clinical trials.

PNS is the major component of Xuesaitong, a very widely used Chinese patent medicine, whose mainly pharmacological effect is improving microcirculation. Besides, several studies including our previous study had proved its function in anti-osteoporosis,[24,25,35] but no studies have investigated its function in IDD. The present study demonstrated for the first time that appropriate doses of PNS can effectively inhibit EP degeneration and attenuate the decline of IVD volume. However, because there was only one observation time point in our experiment, it's still unclear whether the effects seen are restorative or preventative, and further in vivo study based on middle and later stage of IDD model is required.

Our in vitro study revealed that PNS effectively inhibited RANKL-induced osteoclastic activation and had a boost effect on the expression of transcription factor PAX6. Previous studies have shown that overexpression of PAX6 in osteoclast precursor cells significantly inhibited osteoclastogenesis by selectively inhibiting the p38/MAPK signaling pathway,[42] so the inhibitory effect of PNS on osteoclast formation may be mediated by specific activation of PAX6 and the inhibition of p38/MAPK signaling pathway. However, there are still many questions that need to be further addressed in future studies. For example, the total saponins of Panax notoginseng mainly include ginsenosides Ra3, Rg1, Rb1, Rd, and notoginsenoside R1, and which specific component of PNS plays a major role in inhibiting the osteoclasts activities? Besides, which receptor on the osteoclast and what intracellular signaling pathway are responsible for mediating the activation of PAX6? In addition, does the active component have access to the NP in addition to acting in the EP? We believe that future studies will further explain these remaining questions and provide more molecular evidence for the clinical application of PNS in treating IDD as well as LBP.

5 | CONCLUSION

In summary, we demonstrated that appropriate dose of PNS inhibited the formation of cavities in sclerotic EP, increased IVD volume, and attenuated the degeneration of NP, EP, as well as the whole IVD. Moreover, the inhibition of overactive osteoclast within sclerotic EP may be a key process for PNS to prevent EP porositization, which requires more mechanistic investigation in the future. These findings may provide a potential novel therapeutic strategy for IDD.

AUTHOR CONTRIBUTION

Hao Hu: Conceptualization; research design; methodology; investigation; writing – original draft; writing – review and editing. **Xuenong Zou:** Conceptualization; research design; methodology; resources; writing – review and editing; funding acquisition. **Yan Chen:** Research design; methodology; investigation; writing – original draft; writing – review and editing. **Fangli Huang:** Research design; investigation; writing – original draft; writing – review and editing. **Zemin Ling:** Research design; methodology; writing – review and editing; funding acquisition. **Bolin Chen:** Investigation; formal check and data analysis; writing – review and editing. **Zhiyuan Zou:** Formal check and data analysis; writing – review and editing. **Bizhi Tan:** Formal check and data analysis; writing – review and editing. **Chun Liu:** Resources; writing – review and editing. **Hualin Yi:** Resources; writing – review and editing. **Yong Wan:** Resources; writing – review and editing.

ORCID

Hao Hu https://orcid.org/0000-0002-1127-0589

REFERENCES

1. Knezevic NN, Candido KD, Vlaeyen JWS, Van Zundert J, Cohen SP. Low back pain. *Lancet*. 2021;*398*(10294):78-92.
2. Hartvigsen J, Hancock MJ, Kongsted A, et al. What low back pain is and why we need to pay attention. *Lancet*. 2018;*391*(10137):2356-2367.
3. Luoma K, Riihimäki H, Luukkonen R, Raininko R, Viikari-Juntura E, Lamminen A. Low back pain in relation to lumbar disc degeneration. *Spine (Phila pa 1976)*. 2000;*25*(4):487-492.
4. Kamali A, Ziadlou R, Lang G, et al. Small molecule-based treatment approaches for intervertebral disc degeneration: current options and future directions. *Theranostics*. 2021;*11*(1):27-47.
5. Boubriak OA, Watson N, Sivan SS, Stubbens N, Urban JPG. Factors regulating viable cell density in the intervertebral disc: blood supply in relation to disc height. *J Anat*. 2013;*222*(3):341-348.
6. Fournier DE, Kiser PK, Shoemaker JK, Battié MC, Séguin CA. Vascularization of the human intervertebral disc: a scoping review. *JOR Spine*. 2020;*3*(4):e1123.
7. Blanquer SB, Grijpma DW, Poot AA. Delivery systems for the treatment of degenerated intervertebral discs. *Adv Drug Deliv Rev*. 2015;*84*:172-187.
8. Roberts S, Menage J, Urban JP. Biochemical and structural properties of the cartilage end-plate and its relation to the intervertebral disc. *Spine (Phila pa 1976)*. 1989;*14*(2):166-174.
9. Chen C, Zhou T, Sun X, et al. Autologous fibroblasts induce fibrosis of the nucleus pulposus to maintain the stability of degenerative intervertebral discs. *Bone Res*. 2020;*8*:7.
10. Hodgkinson T, Shen B, Diwan A, Hoyland JA, Richardson SM. Therapeutic potential of growth differentiation factors in the treatment of degenerative disc diseases. *JOR Spine*. 2019;*2*(1):e1045.
11. Ling Z, Li L, Chen Y, et al. Changes of the end plate cartilage are associated with intervertebral disc degeneration: a quantitative magnetic resonance imaging study in rhesus monkeys and humans. *J Orthop Translat*. 2020;*24*:23-31.
12. Dudli S, Fields AJ, Samartzis D, Karppinen J, Lotz JC. Pathobiology of Modic changes. *Eur Spine J*. 2016;*25*(11):3723-3734.
13. Torkki M, Majuri ML, Wolff H, et al. Osteoclast activators are elevated in intervertebral disks with Modic changes among patients

operated for herniated nucleus pulposus. *Eur Spine J*. 2016;*25*(1): 207-216.

14. Liu S, Sun Y, Dong J, Bian Q. A mouse model of lumbar spine instability. *J Vis Exp*. 2021;*2021*(170):e61722.

15. Ashinsky BG, Bonnevie ED, Mandalapu SA, et al. Intervertebral disc degeneration is associated with aberrant endplate remodeling and reduced small molecule transport. *J Bone Miner Res*. 2020;*35*(8):1572-1581.

16. Ni S, Ling Z, Wang X, et al. Sensory innervation in porous endplates by Netrin-1 from osteoclasts mediates PGE2-induced spinal hypersensitivity in mice. *Nat Commun*. 2019;*10*(1):5643.

17. Wang T, Guo R, Zhou G, et al. Traditional uses, botany, phytochemistry, pharmacology and toxicology of Panax notoginseng (Burk.) F.H. Chen: a review. *J Ethnopharmacol*. 2016;*188*:234-258.

18. Peng XX, Zhang SH, Wang XL, et al. Panax Notoginseng flower saponins (PNFS) inhibit LPS-stimulated NO overproduction and iNOS gene overexpression via the suppression of TLR4-mediated MAPK/NF-kappa B signaling pathways in RAW264.7 macrophages. *Chin Med*. 2015;*10*:15.

19. Luo H, Vong CT, Tan D, et al. Panax notoginseng saponins modulate the inflammatory response and improve IBD-like symptoms via TLR/-NF-κB and MAPK signaling pathways. *Am J Chin Med*. 2021;*49*(4): 925-939.

20. Ng TB, Liu F, Wang HX. The antioxidant effects of aqueous and organic extracts of Panax quinquefolium, Panax notoginseng, Codonopsis pilosula, Pseudostellaria heterophylla and Glehnia littoralis. *J Ethnopharmacol*. 2004;*93*(2–3):285-288.

21. Lau AJ, Toh DF, Chua TK, Pang YK, Woo SO, Koh HL. Antiplatelet and anticoagulant effects of Panax notoginseng: comparison of raw and steamed Panax notoginseng with Panax ginseng and Panax quinquefolium. *J Ethnopharmacol*. 2009;*125*(3):380-386.

22. Dong TTX, Cui XM, Song ZH, et al. Chemical assessment of roots of Panax notoginseng in China: regional and seasonal variations in its active constituents. *J Agric Food Chem*. 2003;*51*(16):4617-4623.

23. Liu H, Yang J, du F, et al. Absorption and disposition of ginsenosides after oral administration of Panax notoginseng extract to rats. *Drug Metab Dispos*. 2009;*37*(12):2290-2298.

24. Wenxi D, Shufang D, Xiaoling Y, Liming Y. Panax notoginseng saponins suppress radiation-induced osteoporosis by regulating bone formation and resorption. *Phytomedicine*. 2015;*22*(9):813-819.

25. Hu H, Chen Y, Zou Z, et al. Panax Notoginseng Saponins prevent bone loss by promoting angiogenesis in an osteoporotic mouse model. *Biomed Res Int*. 2020;*2020*:1-8.

26. Jang Y, Kim M, Ko S. N-Butanol extracts of Panax notoginseng suppress LPS-induced MMP-2 expression in periodontal ligament fibroblasts and inhibit osteoclastogenesis by suppressing MAPK in LPS-activated RAW264.7 cells. *Arch Oral Biol*. 2011;*56*(11):1319-1327.

27. Reagan-Shaw S, Nihal M, Ahmad N. Dose translation from animal to human studies revisited. *FASEB J*. 2008;*22*(3):659-661.

28. Lee SE, Woo KM, Kim SY, et al. The phosphatidylinositol 3-kinase, p38, and extracellular signal-regulated kinase pathways are involved in osteoclast differentiation. *Bone*. 2002;*30*(1):71-77.

29. Melgoza IP, Chenna SS, Tessier S, et al. Development of a standardized histopathology scoring system using machine learning algorithms for intervertebral disc degeneration in the mouse model-An ORS spine section initiative. *JOR Spine*. 2021;*4*(2):e1164.

30. Ji Z, Cheng Y, Yuan P, Dang X, Guo X, Wang W. Panax notoginseng stimulates alkaline phosphatase activity, collagen synthesis, and mineralization in osteoblastic MC3T3-E1 cells. *In Vitro Cell Dev Biol Anim*. 2015;*51*(9):950-957.

31. Chen B, Li XD, Liu DX, et al. Canonical Wnt signaling is required for Panax notoginseng saponin-mediated attenuation of the RANKL/OPG ratio in bone marrow stromal cells during osteogenic differentiation. *Phytomedicine*. 2012;*19*(11):1029-1034.

32. Rodriguez AG, Rodriguez-Soto AE, Burghardt AJ, Berven S, Majumdar S, Lotz JC. Morphology of the human vertebral endplate. *J Orthop Res*. 2012;*30*(2):280-287.

33. Taher F, Essig D, Lebl DR, et al. Lumbar degenerative disc disease: current and future concepts of diagnosis and management. *Adv Orthop*. 2012;*2012*:970752.

34. Bian Q, Jain A, Xu X, et al. Excessive activation of TGFbeta by spinal instability causes vertebral endplate sclerosis. *Sci Rep*. 2016;*6*:27093.

35. Fan JZ, Wang Y, Meng Y, et al. Panax notoginseng saponins mitigate ovariectomy-induced bone loss and inhibit marrow adiposity in rats. *Menopause*. 2015;*22*(12):1343-1350.

36. Ortiz AO, Bordia R. Injury to the vertebral endplate-disk complex associated with osteoporotic vertebral compression fractures. *AJNR Am J Neuroradiol*. 2011;*32*(1):115-120.

37. Che-Nordin N, Deng M, Griffith JF, et al. Prevalent osteoporotic vertebral fractures more likely involve the upper endplate than the lower endplate and even more so in males. *Ann Transl Med*. 2018;*6*(22):442.

38. Siemionow K, An H, Masuda K, Andersson G, Cs-Szabo G. The effects of age, sex, ethnicity, and spinal level on the rate of intervertebral disc degeneration: a review of 1712 intervertebral discs. *Spine (Phila pa 1976)*. 2011;*36*(17):1333-1339.

39. Wang YX, Griffith JF, Ma HT, et al. Relationship between gender, bone mineral density, and disc degeneration in the lumbar spine: a study in elderly subjects using an eight-level MRI-based disc degeneration grading system. *Osteoporos Int*. 2011;*22*(1):91-96.

40. O'Connell GD, Vresilovic EJ, Elliott DM. Comparison of animals used in disc research to human lumbar disc geometry. *Spine (Phila pa 1976)*. 2007;*32*(3):328-333.

41. Alini M, Eisenstein SM, Ito K, et al. Are animal models useful for studying human disc disorders/degeneration? *Eur Spine J*. 2008;*17*(1):2-19.

42. Jie Z, Shen S, Zhao X, et al. Activating β-catenin/Pax6 axis negatively regulates osteoclastogenesis by selectively inhibiting phosphorylation of p38/MAPK. *FASEB J*. 2018;*33*(3):4236-4247.

SUPPORTING INFORMATION

Additional supporting information may be found in the online version of the article at the publisher's website.